Apparent Permeability Model of Coalbed Methane in Moist Coal: Coupling Gas Adsorption and Moisture Adsorption

Zhigao Peng,* Shenggui Liu, Zongwei Deng, Haoxiong Feng, and Ming Xiao

| ACCESS | | �</> Metrics & More | | 📰 Article Recommendations |

ABSTRACT: Under specific conditions, moisture in natural coal seams can be adsorbed in the pores of the coal matrix, reducing the amount of methane adsorption sites and the effective area of the transport channels. This makes the prediction and evaluation of permeability in CBM exploitation more challenging. In this paper, we developed an apparent permeability model of coalbed methane coupling viscous flow, Knudsen diffusion, and surface diffusion which considers the effects of adsorbed gas and moisture in the pores of the coal matrix on the permeability evolution. The predicted data of the present model are compared with those of other models, and the results show good agreement, verifying the accuracy of the model. The model was employed to study the apparent permeability evolution characteristics of coalbed methane under different pressure and pore size distribution conditions. The main findings are as follows: (1) moisture content increases with saturation, with a slower increase for smaller porosities and an accelerated non-linear increase for porosities greater than 0.1. (2) Gas adsorption in pores decreases permeability, further weakened by moisture adsorption under high pressure but negligible at pressures below 1 MPa. (3) Higher water saturation weakens gas transport capacity, especially with pore sizes smaller than 10 nm. (4) The non-Darcy effect weakens with higher initial porosity, and neglecting moisture adsorption may significantly deviate from actual values in modeling methane transport in coal seams. The present permeability model can capture the transport characteristics of CBM in moist coal seams more realistically and is more applicable for predicting and evaluating the gas transport performance under dynamic variations of pressure, pore size, and moisture. The results in this paper can explain the transport behavior of gas in moist, tight, porous media and also provide a foundation for coalbed methane permeability evaluation.
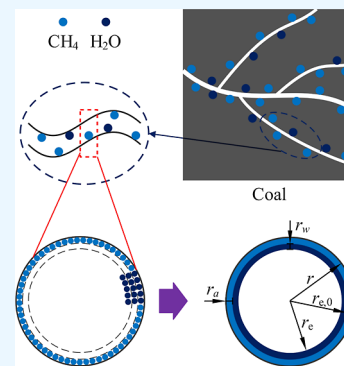
1. INTRODUCTION

Coalbed methane (CBM) is a typical unconventional natural gas with the primary component of methane, which is confined in the reservoir under specific temperatures and pressures. The exploitation and utilization of CBM can simultaneously achieve the triple aims of energy utilization, low-carbon environmental protection, and coal mine safety; therefore, it has received wide attention in recent years. Different from conventional natural gas, CBM is stored in coal seams in many ways, such as adsorption, free-flow, dissolution, etc. The transport of CBM during exploitation is a complicated process governed by multiple factors, and understanding the permeability of CBM in coal seams is a crucial issue in the study of CBM migration performance, which is also of great significance for the accurate prediction and evaluation of CBM transport properties and production capacity.

Coal is a type of tight porous medium with the pore size distribution in the range of 1 to 100 nm, making the traditional Darcy's law no longer available for fluid flow in it. There have been many related studies on the non-Darcy effect for gas migration in nanopores. Beskok and Karniadakis[1] proposed a unified model based on the Hagen−Poiseuille equation for describing the gas flow in a single capillary which considers the essential flow regimes in tight porous media, involving

continuous, slip, transition, and free molecular flows. However, it is only applicable to the case where the Knudsen number is less than or equal to 1. Xiong[2] further investigated the impact of gas adsorption and surface diffusion on the evolution of apparent permeability by considering the mass transfer process of adsorbed gas. Freeman[3] employed a dusty gas model (DGM) to explain the Knudsen diffusion of gas in the reservoir. Kang[4] adopted different weighting factors or linear summation to introduce the combined effect of gas slippage and Knudsen diffusion. These weighting factors were further developed by Wu[5,6] and took into account the impact of surface diffusion in addition to viscous flow and Knudsen diffusion. The layer of gas molecules adsorbed on the surface within the pores in the coal matrix, which has several nanopores, lowers the real extent of the transport channel. Thus, when predicting the apparent
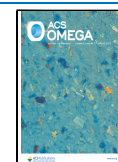
permeability of CBM, the impact of the adsorbed layer of gas molecules should be taken into account.[7−11]

In summary, it can be seen that the existing permeability models are mainly superimposed by considering the contributions of viscous flow, Knudsen diffusion, transition flow, free molecular flow, and surface diffusion to the total flux through the Knudsen number. However, many studies have shown that the presence of inherent moisture in in situ reservoirs can affect the adsorption and transport ability of CH_4. In 1936, when Coppens studied the adsorption characteristics of Belgian coal, he discovered that the potential of coal to adsorb methane decreases when moisture is present. Several academics have studied the properties of moist coal for gas adsorption since the 1970s.[12] It is commonly accepted that coal's ability to absorb gases declines as moisture content rises. However, the gas adsorption capacity does not change when the moisture content surpasses a threshold level.[13] Joubert[14] further revealed that the oxygen content in coal regulates the moisture content's critical value. Wang[15] reported that the presence of moisture occupies a portion of the pore space and diminishes the gas adsorption sites of coal, which lowers the amount of gas adsorption. Recent studies[16−20] have shown that the Langmuir volume drops with increasing intrinsic moisture content, and the exponential equation may be used to describe the relationship between the amount of methane adsorption and intrinsic moisture content.

The impact of moisture on the gas adsorption capacity of coal is related to the coal rank. Laxminarayana[21] showed that the maximum gas adsorption capacity of dry coal changed in a U-shape with increasing coal rank, while the maximum gas adsorption capacity of moist coal increased slightly. According to Day,[22] low-rank coals are more sensitive to moisture than high-rank coals. GUO[23] found experimentally that moisture would dramatically reduce the gas adsorption capacity of low-rank coals. The amount of inhibition increases as moisture content rises, but the increment of inhibition gradually decreases, and the exponential formula can better fit the data on the gas adsorption capacity of low-rank coals with the variation of moisture content.

In summary, most previous permeability models have predicted and evaluated the transport performance of gases in tight coal seams with extensive pore size coverage by coupling viscous flow (considering gas slip effects) and Knudsen diffusion to the total flow flux. Some researchers have further considered the contribution of surface diffusion of adsorbed molecules to the flow flux, or the decay in transport performance caused by gases adsorbing in the pore. However, natural coal seams are rich in moisture, the accompanying variation in moisture content during CBM development further complicates the transport behavior of CBM, and the impact of the presence of moisture on gas transport capacity is not considered in all these models.

To more realistically capture the transport behavior of CBM in moist coal seams, this paper further develops an apparent permeability prediction model for CBM transport in naturally moist coal, based on the model developed by the previous authors. The model couples the contributions of viscous flow (considering the gas slip effect), Knudsen diffusion, and surface diffusion to the total flow flux, considering the effects of gas and moisture adsorption on the transport capacity, and further introduces an exponential formula based on the findings of previous isothermal adsorption experiments to describe the decay of gas adsorption and adsorption capacity with changes in the moisture content of the coal matrix, which can be more applicable for predicting and evaluating the gas transport

performance with dynamically variable pressure, pore size, and moisture content.

2. APPARENT PERMEABILITY MODEL FOR GAS TRANSPORT IN MOISTURE-POROUS MEDIA

Pores in typical coal have a large amount of gas adsorbed on the surface and are generally less than 100 nm in diameter.[24−28] In nanoscale pores, the probability that the gas molecules collide with the wall of the pore is significantly increased, providing a non-negligible source of momentum for gas transfer near the pore wall, which deviates markedly from the results calculated based on Darcy's law.[10,29] These will bring two new challenges to modeling. On the one hand, gas slip provides an additional contribution to the total flow, and on the other hand, the importance of gas Kundsen diffusion becomes prominent as one of the main flow regimes. What is more, the adsorption of gas molecules and moisture in nanopores adds more complexity to the exploration of methane migration characteristics. First, gas molecules adsorbed on the pore surface are driven by the concentration difference to pass along the adsorption layer; second, the layer of molecules adsorbed on the pore wall will occupy the volume of the pore space and reduce the effective area of the migration channel. Furthermore, the inherent moisture present in the natural coal seam will also adsorb onto the pore surface, and the adsorbed moisture will occupy the adsorption sites, leading to the decay of the real adsorption capacity of the coal matrix and the schematic illustration of the mode of gas and moisture transfer in the moist coal, as shown in Figure 1. All of the above factors are pressure-dependent, and
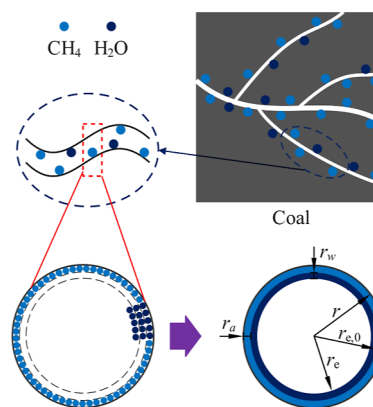

Figure 1. Schematic illustration of the mode of gas and moisture transfer in moist coal.

therefore, neglecting these aspects when modeling the permeability of methane migration in natural coal seams can result in systematic errors that vary with gas pressure.

2.1. Flux Contributed by Viscous Flow in a Moist Porous Media. For fluid flow in a capillary with a radius r, the intrinsic permeability K_∞ can be obtained based on Poiseuille's law

$$K_\infty = \frac{r^2}{8} \tag{1}$$

The corresponding total volumetric flux Q_∞ is

$$Q_\infty = \pi r^2 \frac{K_\infty}{\mu} \nabla p \tag{2}$$

where p is the pressure, and μ is the gas dynamic viscosity coefficient.

When the adsorption between gases and the wall of capillaries within porous media occurs, the reduction of the effective area for free gas transfer may be enlarged.[2] Assuming that the gas adsorption is following the Langmuir adsorption theory, the amount of gas adsorbed will be a function of pressure. The coverage of the adsorbed gas molecules on the capillary surface under pressure p is

$$\theta = \frac{V_s}{V_L} = \frac{p}{p + P_L} \tag{3}$$

where V_s is the adsorption amount, V_L is the Langmuir volume, and P_L is the Langmuir pressure.

After deducting the space occupied by the adsorbed gas molecules with a diameter d_m, the effective radius of the capillary $r_{e,0}$ for the free gas flow can be obtained

$$r_{e,0} = r - d_m\theta \tag{4}$$

When taking into account the adsorption of capillaries with moisture, the effective radius r_e should be rewritten as

$$r_e = r - d_m\theta - r_w \tag{5}$$

where r_w is the equivalent radius of the adsorption layer of water.

Considering the gas adsorption layer, the relationship between the effective radius and the initial radius is

$$\phi_0 = \frac{r_{e,0}^2}{r^2} \tag{6}$$

After further consideration of moisture adsorption, the relationship can be modified as

$$\phi = \frac{r_e^2}{r^2} = \frac{\varepsilon_e}{\varepsilon_0} \tag{7}$$

As shown in Figure 1, the water saturation S_w can be written as[30]

$$S_w = \frac{(r - d_m\theta)^2 - (r - d_m\theta - r_w)^2}{r^2} \tag{8}$$

Moisture adsorption occupies adsorption sites on the capillary surface, resulting in the decay of gas adsorption capacity. The exponential decay equation can be employed to describe the effect of moisture on gas adsorption capacity[20]

$$V_L = V_{Lg} + V_{Lw}\exp(-\varphi\omega), \quad 0 < \omega < \omega_c \tag{9}$$

where φ is the decay coefficient of Langmuir volume, the value of which is related to the composition of the coal and can be obtained from the experiment, ω is the mass moisture content, which is the ratio of the total mass of water to the total mass of the dried material, ω_c is the threshold of moisture content, beyond which the maximum adsorption capacity is not affected by the further growth of moisture, and V_{Lg} and V_{Lw} are the maximum adsorption capacities of unique adsorption sites for gases and gas adsorption sites with moisture adsorption potential, respectively.

By analyzing the volume relationship among solids, pores, and water in moist coal, the mass moisture content can be obtained

$$\omega = \frac{\varepsilon S_w \rho_w}{\rho_s - \varepsilon S_w \rho_w} \tag{10}$$

where ρ_s and ρ_w are the densities of the moist coal and the water adsorption layer, respectively.

Chen[16] found experimentally that the Langmuir pressure is related to the moisture content. Day[22] and Ozdemir[31] showed that moisture can change the heat of adsorption. Based on the exponential decay equation, Chen[19] further proposed a relationship between the Langmuir pressure and the moisture content

$$P_L = P_{Lg} + P_{Lw}\exp(-\xi\omega) \tag{11}$$

where P_{Lg} is the pressure constant unaffected by moisture, P_{Lw} is the fraction that can be affected by moisture adsorption, and ξ is a weighting factor representing the role of moisture in gas adsorption.

The volumetric flux contributed by the viscous flow of gas can be expressed as

$$Q_{a,\infty} = \pi r_e^2 \frac{r_e^2}{8\mu}\nabla p = \pi r^2 \phi \frac{r_e^2}{8\mu}\nabla p \tag{12}$$

Permeability becomes a pressure-dependent function

$$K_{a,\infty} = \phi(p)\frac{r_e^2(p)}{8} \tag{13}$$

2.2. Flux Contribution by the Knudsen Diffusion in a Moist Porous Media.

Due to the extreme confinement of the pore space, methane flows in the coal matrix in a transitional or slip flow regime. The Navier−Stokes (N−S) equation with appropriate slip boundary conditions is sufficient for mathematical modeling in the slip flow regime. However, in transition flows, where the mean free path of the gas molecules is comparable to the pore diameter, the momentum transfer between the gas molecules and between the gas molecules and the pore wall is equally important. Therefore, in the case of transition flow, the combined effect of viscous flow and Knudsen diffusion must be taken into account.[6,32]

When the Knudsen number is $10^{-3} < Kn < 10^{-1}$, the gas intermolecular collision is dominant, the collision probability between the gas molecules, the wall is small but cannot be neglected, the velocity of the gas molecules near the wall is non-zero, the slip effect will occur, and the gas transfer at that moment is the slip flow, which can be described by the ideal gas slip flow equation.[32] At present, most of the studies in the relevant aspects employ the Klinkenberg equation for modification.[33]

$$K = K_\infty f(Kn) = K_\infty\left(1 + \frac{b_k}{p}\right) \tag{14}$$

where $f(Kn)$ is Klinkenberg's correction factor, which is a first-order correction, Beskok and Karniadakis[1] gave a second-order correction applicable to describe four flow regimes (viscous flow, slip flow, transition flow, and free molecular flow)

$$f(Kn) = (1 + \alpha Kn)\left(1 + \frac{4Kn}{1 - bKn}\right) \tag{15}$$

where b is the coefficient for gas slippage, generally taken as $b = -1$; $\alpha(Kn)$ is the rarefaction coefficient, given by Civan[34]

$$\alpha = \frac{1.358}{1 + 0.178Kn^{-0.4348}} \tag{16}$$

The Knudsen number is defined as the ratio of the mean free path of molecules to the characteristic pore size of the media

$$Kn = \frac{\lambda}{r} \tag{17}$$

where the mean free path of the gas molecule is

$$\lambda = \frac{\mu}{p}\sqrt{\frac{\pi RT}{2M}} \tag{18}$$

When the effect of both the gas adsorption layer and moisture adsorption is taken into account, the effective radius r_e should be adopted; then, the permeability should be corrected to

$$K_a = K_{a,\infty}(p)f(Kn') \tag{19}$$

The total mass flux is

$$m_a = \rho\pi r^2 \frac{K_a}{\mu}\nabla p = \rho\pi r^2 \frac{K_a}{\mu}\nabla p \tag{20}$$

When $Kn > 10$, the collision of the gas molecules with the wall surface of the nanopore is dominant, and the gas transport is Knudsen diffusion, which can be described by the ideal gas Knudsen diffusion equation.[34] The flux contributed by Knudsen diffusion can be obtained based on Fick's law

$$J_{Kn} = -D_{Kn}\nabla C \tag{21}$$

Roy[35] gave the equivalent form of Knudsen diffusion in nanopores

$$J_{Kn} = -D_{Kn}\frac{1}{RT}\nabla p \tag{22}$$

where D_{Kn} is the Knudsen diffusion coefficient, and the gas flow through a single capillary can be defined as[36]

$$D_{Kn} = \frac{2r_e}{3}\sqrt{\frac{8RT}{\pi M}} \tag{23}$$

Therefore, the mass flux contributed by Knudsen diffusion can be expressed as

$$m_{Kn} = \pi r_e^2 D_{Kn}\frac{M}{RT}\nabla p = \pi r^2 \phi D_{Kn}\frac{M}{RT}\nabla p \tag{24}$$

2.3. Fluxes Contributed by Surface Diffusion in Moist Porous Media.

When the gas flows in the capillary, the free gas and adsorbed gas exchange positions, resulting in inconsistent concentrations in the adsorption layer of the gas, and the adsorbed gas passes along the adsorption layer driven by the concentration difference, which is the so-called surface diffusion. The flux contributed by surface diffusion can be obtained based on the Langmuir isothermal adsorption equation

$$J_s = -D_s\nabla C_a = -D_s\frac{C_{max}P_L}{(p + P_L)^2}\nabla p \tag{25}$$

The surface diffusion coefficient is a function of temperature, surface gas concentration, and adsorbent/solid surface interaction.[37] Based on the transition state theory, Chen[38] proposed a surface diffusion coefficient

$$D_s = D_{s0}f(\theta) \tag{26}$$

$$f(\theta) = \frac{1 - \theta + \frac{s}{2}(2\theta - \theta^2) + \mathbf{H}(1 - s)\frac{(s - s^2)}{2}\theta^2}{(1 - \theta + s\theta/2)^2} \tag{27}$$

$$\mathbf{H}(1 - s) = \begin{cases} 0, & s \geq 1 \\ 1, & 0 \leq s < 1 \end{cases} \tag{28}$$

where D_{s0} is the surface diffusion coefficient as the coverage is zero, which depends on the temperature and gas activation energy, $\mathbf{H}(1 - s)$ is a Heaviside function, and s is a quantity that measures the degree to which the pores are clogged by adsorbed molecules, taken as $s = 0.5$.

Therefore, the mass flux that surface diffusion contributes is

$$m_s = D_s\frac{MC_{max}P_L}{(p + P_L)^2}\pi(r^2 - r_{e,0}^2)\nabla p$$
$$= \pi r^2 D_s\frac{MC_{max}P_L}{(p + P_L)^2}(1 - \phi_0)\nabla p \tag{29}$$

It should be noted that surface diffusion occurs only in the gas adsorption layer; therefore, the effective radius of the considered gas adsorption layer is employed in eq 4.

2.4. Total Flux and Apparent Permeability in Moist Porous Media.

The total mass flux in moist porous media, after superimposing the weights of the fluxes contributed by multiple flow regimes and considering the effects of porosity and tortuosity of porous media, can be expressed as

$$m = \omega_v m_a + \omega_k m_{Kn} + m_s$$
$$= \frac{\rho\pi r^2}{\mu}\nabla p\left[\frac{1}{1 + Kn}\frac{\varepsilon_0}{\tau}K_a + \frac{1}{1 + 1/Kn}\frac{\mu}{\rho}\frac{\phi\varepsilon_0}{\tau}D_{Kn}\frac{M}{RT}\right.$$
$$\left. + D_s\frac{\mu}{\rho}\frac{MC_{max}P_L}{(p + P_L)^2}\frac{\varepsilon_0}{\tau}(1 - \phi_0)\right] \tag{30}$$

Viscous flow and Knudsen diffusion require individual weighting factors to determine their respective contributions to the total flow,[36,39] and from the analysis of collision frequencies between gas molecules and between molecules and pore walls, Wu[5,6] obtained the weighting factors to distinguish the contributions of these two flow regimes to the total flow flux.

$$\omega_v = 1/(1 + Kn), \quad \omega_k = 1/(1 + 1/Kn), \quad \omega_v + \omega_k = 1 \tag{31}$$

Therefore, the apparent permeability of coalbed methane migration in moist coal can be expressed as

$$K_{app,om} = \frac{1}{1 + Kn}\frac{\varepsilon_0}{\tau}K_a + \frac{1}{1 + 1/Kn}\frac{\mu}{\rho}\frac{\phi\varepsilon_0}{\tau}D_{Kn}\frac{M}{RT}$$
$$+ D_s\frac{\mu}{\rho}\frac{MC_{max}P_L}{(p + P_L)^2}\frac{\varepsilon_0}{\tau}(1 - \phi_0) \tag{32}$$

The present permeability model can capture the transport characteristics of CBM in moist coal seams more realistically and is more applicable for predicting and evaluating the gas transport performance under dynamic variations of pressure, pore size, and moisture. However, the permeability model does not include the effects of adsorption hysteresis and stress changes in the process of adsorption and desorption, which will be considered in our future study.

3. RESULTS AND DISCUSSION

3.1. Relationship Between the Characteristic Parameters of Moisture Coal.

The porosity, water content, Langmuir volume, and Langmuir pressure of coal seams vary
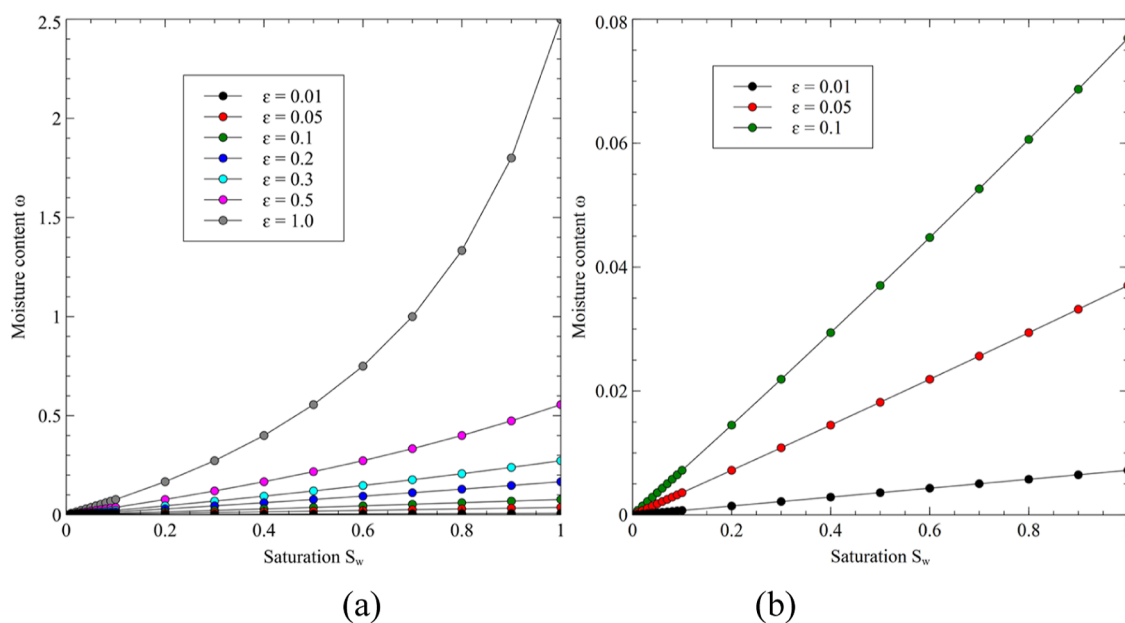
Figure 2. Relationship between moisture content and saturation under different initial porosity. (a) Porosity of the coal seam with a wide extent and (b) porosity of the typical coal seam.
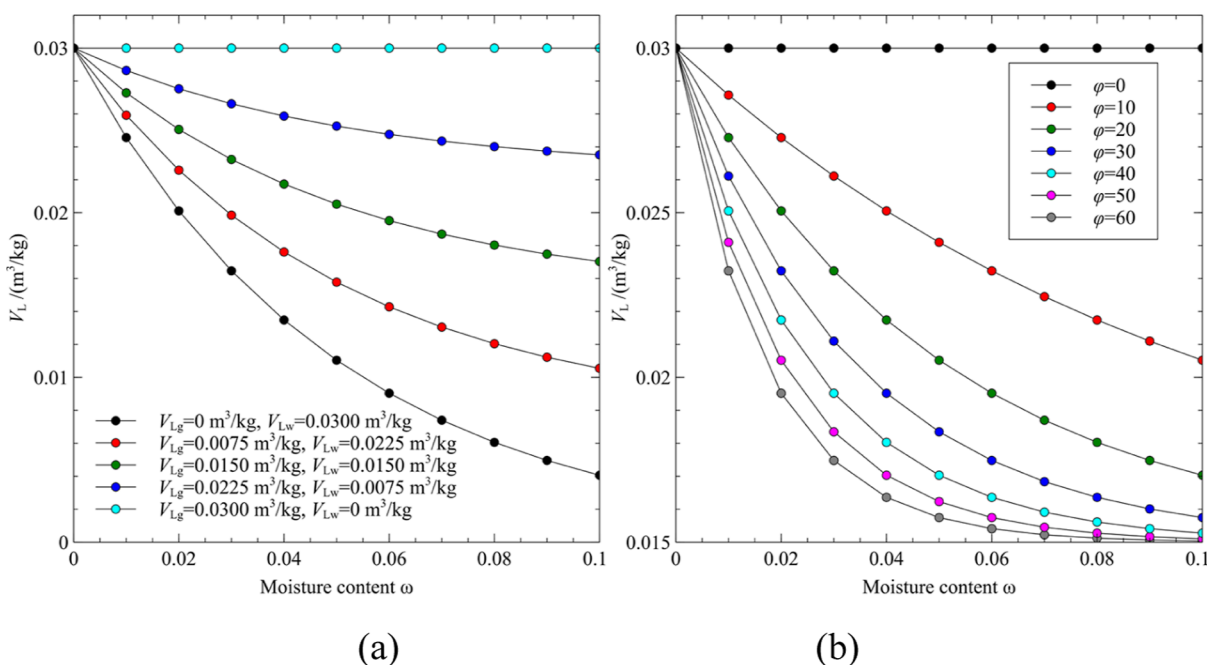

Figure 3. Relationship between Langmuir volume and moisture content. (a) Under different V_{Lg} and V_{Lw} and (b) under different φ.

widely depending on the type, location, and maturation of the coal, etc. Some studies have shown that the inherent moisture content of coal varies with different magnitudes of maturation. Generally, the moisture range of lignite is 10−28%, that of long-flame coal is 3−12%, and that of anthracite is lower.[40,41] It is essential to analyze the relationship between porosity, saturation, moisture content, Langmuir volume, and Langmuir pressure to explain the evolution of apparent permeability.

From Figure 2a, it can be found that the moisture content ω grows with the increase of saturation S_w, and when the porosity is small, the growth rate of ω is slow, and when $\varepsilon > 0.1$, the growth rate of ω is greatly accelerated, and the growth trend begins to show nonlinear characteristics. The porosity of a typical coal

seam is usually less than 0.1, and the moisture content is generally positively related to the saturation, as shown in Figure 2b, and the moisture content is maintained at a low level, e.g., 0.69% at a porosity of 0.1 and a saturation of 20%.

Figure 3a shows the results at $\varphi = 20$ and an initial Langmuir volume $V_L = 0.03$ m³/kg. It can be found that V_L is constant for $V_{Lg} = 0.03$ m³/kg and $V_{Lw} = 0$ m³/kg. When V_{Lw} is greater than 0, the Langmuir volume V_L of moist coal decays with the growth of ω. The larger the V_{Lw}, the more the number of adsorption sites affected by moisture adsorption and the more rapidly it decays, and in the limit case, the V_L decay can reach 86.5%. For each of the coal samples, the two parameters, V_{Lg} and V_{Lw}, are different, and the exact values can be obtained by fitting the experimental
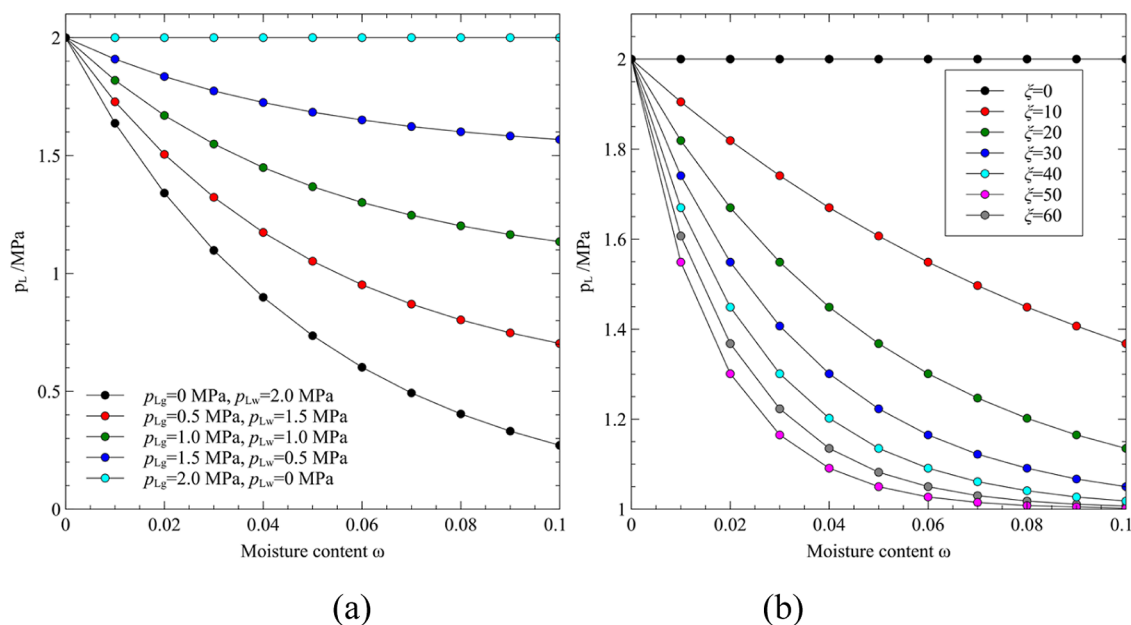
(a)   (b)

Figure 4. Relationship between Langmuir pressure and moisture content. (a) Under different P_{Lg} and P_{Lw} and (b) under different ξ.

data. Figure 3b shows the results for $V_{Lg} = V_{Lw} = 0.015$ m^3/kg, which reflect the effect of the parameter φ on the decay of V_L for moist coal. With $\varphi = 0$, V_L is independent of moisture adsorption and remains constant at its initial value; for φ greater than 0, V_L decays with increasing ω, and the decay rate becomes greater with increasing φ. The value of φ is the key parameter that determines the critical value of V_L decay, and the larger the value of φ, the higher the critical value.

Figure 4a,b show the results for $\xi = 20$, at an initial Langmuir pressure of $P_L = 2$ MPa and $P_{Lg} = P_{Lw} = 1$ MPa, respectively, which present a trend similar to that of V_L in Figure 3. For $P_{Lg} = 2$ MPa and $P_{Lw} = 0$ MPa, P_L does not vary with moisture content; when P_{Lw} is greater than 0, P_L decays with the growth of ω, and the larger P_{Lw} is, the faster the decay rate of P_L. At $\xi = 0$, P_L is independent of moisture adsorption and does not change with ω; as ξ is greater than 0, P_L decays with the growth of ω, and the larger ξ is, the faster the decay rate is, and the decay increment gradually decreases. The decay of P_L also has a critical value, which is governed by the value of ξ.

In engineering, the values of V_{Lg}, V_{Lw}, φ, P_{Lg}, P_{Lw}, and ξ can be obtained by fitting to experimental data, and for specific coal, the combination and superposition of the characteristic effects presented by the above parameters can lead to a complex permeability evolution behavior.

3.2. Comparison of the Apparent Permeability Model with Previous Research. Previous studies have proposed numerous apparent permeability equations to describe the gas transport behavior with the coupling of viscous flow, Knudsen diffusion, and surface diffusion in tight porous media, e.g., the model of Wang[7] considers the contribution of viscous flow and Knudsen diffusion to the total flow in tight porous media, and the models of Ning[8] and Sun[9] both consider the contribution of adsorbed layers of gas molecules to the pore space blockage effect. The apparent permeability model developed in this paper is compared with the mentioned models to illustrate its validity, and the parameters of coal and methane in the comparison are shown in Table 1. It should be noted that the gas density and viscosity under different pressures are obtained from an online calculation software (www.peacesoftware.de/).

Table 1. Parameters of Coal and Methane for Comparison

parameters of coal and methane	value
initial porosity, ε_0	0.1
tortuosity, τ	2
temperature, T (K)	303.15
gas molar mass, M (kg/mol)	0.016
water saturation, S_w	0.2
Langmuir volume, V_{Lg} (m^3/kg)	0.005
Langmuir volume, V_{Lw} (m^3/kg)	0.015
Langmuir pressure, P_{Lg} (MPa)	0.5
Langmuir pressure, P_{Lw} (MPa)	1.5
decay coefficient of Langmuir volume, φ	40
decay coefficient of Langmuir pressure, ξ	30
coal density, ρ_s (kg/m^3)	1450
surface diffusion coefficient at zero coverage, D_{s0} (m^2/s)	1×10^{-7}
pore radius, r (nm)	2

Figure 5 shows the variation of K_{app} with pressure under different average pore sizes. Among them, Wang's model considers the effect of surface diffusion of adsorbed gas but does not include the decay of transport capacity when the pore space adsorbs gas; Sun's and Ning's models simultaneously consider the effect of surface diffusion and the effect of the adsorption layer, and only the contributions of surface diffusion are calculated by different coefficients for these two models. It can be seen that all of the models show a tendency for the apparent permeability to decrease with higher pressure. As the average pore size increases, the magnitude of apparent permeability rises. The apparent permeability of all these models is close to 1×10^{-12} m^2 with an average pore size of 1 μm, while the apparent permeability of all models is concentrated in the range of $1 \times 10^{-18} - 1 \times 10^{-20}$ m^2 when the average pore size is 1 nm. The results of the present paper are consistent with other models under different pressure conditions, indicating the validity of the developed apparent permeability models. However, since our model takes into account moisture adsorption, the apparent permeability of the coal matrix with inherent moisture is weakened to some extent, especially under high-pressure
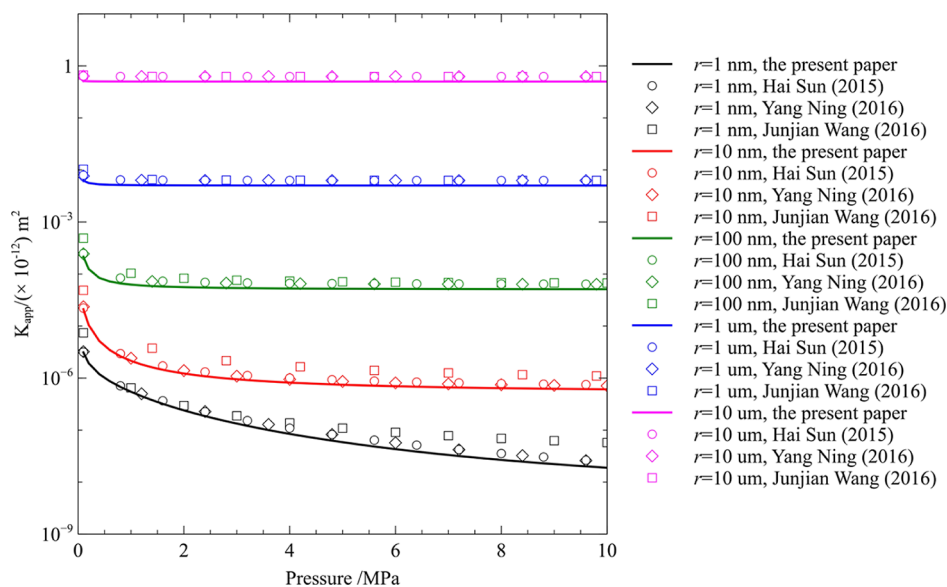
Figure 5. Comparison between the present model and the previous research.

conditions and small-size pores. As a result, the permeability of our model is slightly lower than that of the other models, while the model of Wang,[7] without considering the effect of adsorbed layers of gas molecules, gives a larger permeability than the other models.

3.3. Variation Trend of Apparent Permeability under Different Conditions. The wide distribution of pore size inside coal leads to a significant non-Darcy effect in the process of coalbed methane transport. Previous studies have gradually developed from considering only the viscous flow of gas to a comprehensive coupled model which takes into account viscous flow, Knudsen diffusion, and surface diffusion. In this paper, on these foundations, the effects of gas molecular adsorption and moisture adsorption on the evolution of permeability are considered. Figure 6 shows the trends of K_{app}/K_0 calculated by various models under different pressure conditions, where $K_0 = \varepsilon/\tau K_\infty$, and the value of K_{app}/K_0 can be used to indicate the

magnitude of the non-Darcy effect. Since the pore radius, porosity, and tortuosity of all models in this part are uniform and the calculated values of K_0 are the same, K_{app}/K_0 can also represent the variation of K_{app}. It can be shown that when considering only viscous flow and Knudsen diffusion, K_{app}/K_0 is maintained at a relatively high magnitude for low-pressure conditions, and non-Darcy effects are significant. K_{app}/K_0 drops rapidly with increasing pressure, and at $p = 10$ MPa, K_{app}/K_0 is as low as 0.01 times that for low-pressure conditions. The model including surface diffusion provided a larger K_{app}/K_0 than the other models, indicating that the contribution of surface diffusion to the total flow cannot be ignored, which is in agreement with the findings of Wang.[7] When considering the blocking effect of adsorbed gas molecules on the transport channels, the K_{app}/K_0 values are severely weakened, and compared to the model considering only viscous flow and Knudsen diffusion of gas, the K_{app}/K_0 values are slightly larger at lower pressure and gradually decrease with increasing p. It is because the contribution of surface diffusion to the total gas flow is more significant when the pressure is small, and at higher pressure conditions, the adsorption rate of methane molecules is higher and the channel blockage is more severe, resulting in a smaller K_{app}/K_0. When moisture adsorption is further considered, this trend is more obvious at high pressures, which almost overlap as $p < 1$ MPa, indicating that the effect of moisture adsorption at low pressures is negligible. The above results suggest that surface adsorption increases the magnitude of apparent permeability and enhances the non-Darcy effect, while the adsorption of gas and moisture in the pores decreases the permeability and weakens the non-Darcy effect.

The impact of moisture adsorption on apparent permeability is essentially the dynamic adsorption−desorption process of moisture under different physical and chemical properties of the coal matrix and complex reservoir conditions, which lead to a variation in the effective radius $(r - r_w)/r$ of the pore space channels and the effective transport capacity of CBM. The discussion of the trends of r_w/r under different conditions can provide a foundation for the analysis of the apparent permeability evolution pattern.
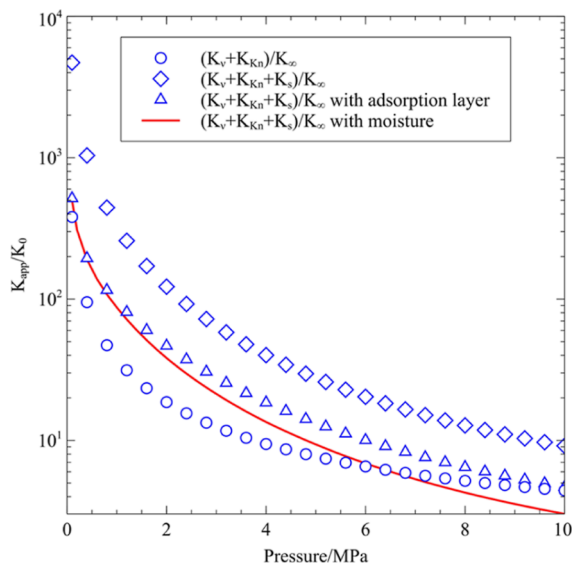

Figure 6. Comparison between the apparent permeability model with different flow regimes.
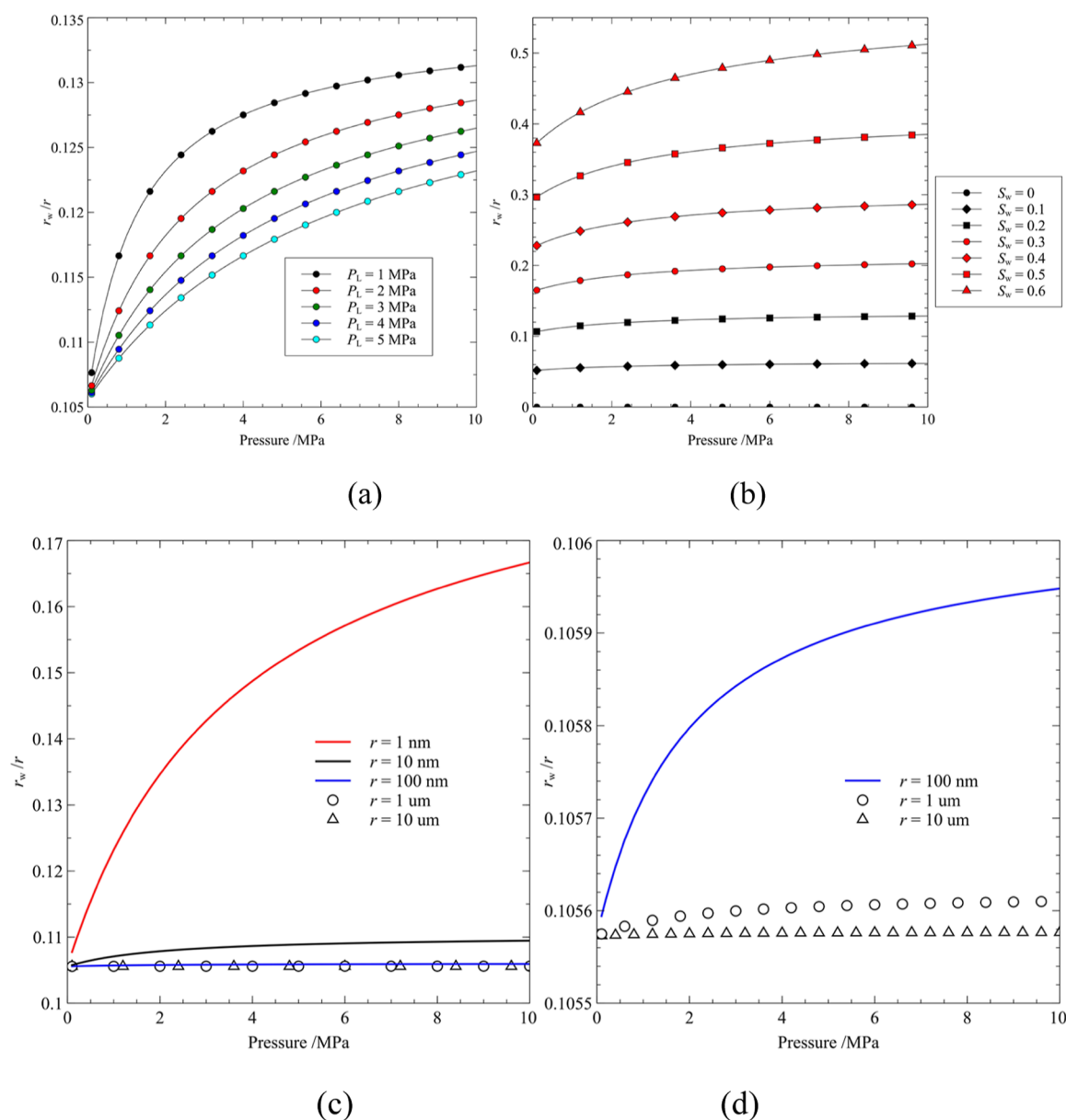
Figure 7. Variation of r_w/r with pressure. (a) Under different P_L, (b) under different S_w, (c) under a wide extent of r, and (d) under conditions of large radius magnitude.

To further investigate the blockage effect of moisture adsorption on the transport channel, Figure 7 shows the trend of r_w/r with p for different P_L, S_w, and r conditions. From the results in Figure 7a, it can be found that with a higher S_w, the initial value of r_w/r is greater, and the growth rate of r_w/r is more rapid, making the blockage effect more significant. For $S_w = 0.6$, the effective area of the transport channel is only 48.8% of the initial value. The results in Figure 7c,d show that with a smaller initial equivalent pore size, when p grows, r_w/r is more sensitive, and the growth rate increases significantly. As r is less than 10 nm, the space occupied by moisture adsorption can reach 10.9% of the total pore volume, and the blockage effect is very significant; for r greater than 1 μm, r_w/r is less sensitive and grows less with p increase.

Figure 8 shows the evolution tendency of K_{app}/K_0 with pressure for different conditions. Figure 8a shows the change of K_{app}/K_0 for different initial porosities. In fact, the larger the initial porosity, the larger K_{app} is when other conditions are

constant. From Figure 8a, it can be found that the higher the initial porosity, the smaller K_{app}/K_0, i.e., the weaker the non-Darcy effect, but the decrease of K_{app}/K_0 becomes less.

The presence of moisture adsorption weakens the capacity of gas transport channels, and the higher the water saturation of the porous media, the lower the K_{app} and the smaller the K_{app}/K_0, as shown in Figure 8b. Figure 8c shows that under low-pressure conditions, the larger the P_L, the lower the K_{app}/K_0. As the pressure grows, the effect of moisture adsorption becomes increasingly significant, leading to the decay of P_L. The greater the value of P_L, the more decay occurs, and K_{app}/K_0 instead becomes greater as P_L increases. However, the phenomenon is related to the magnitude of both P_{Lg} and P_{Lw}, the smaller P_{Lw} is, the less P_L is affected by moisture adsorption, and the tendency of K_{app}/K_0 with P_L may not follow the same trend at high pressure. Although V_L also decays under high-pressure conditions due to moisture adsorption, K_{app}/K_0 generally maintains the tendency to grow with V_L, as shown in Figure
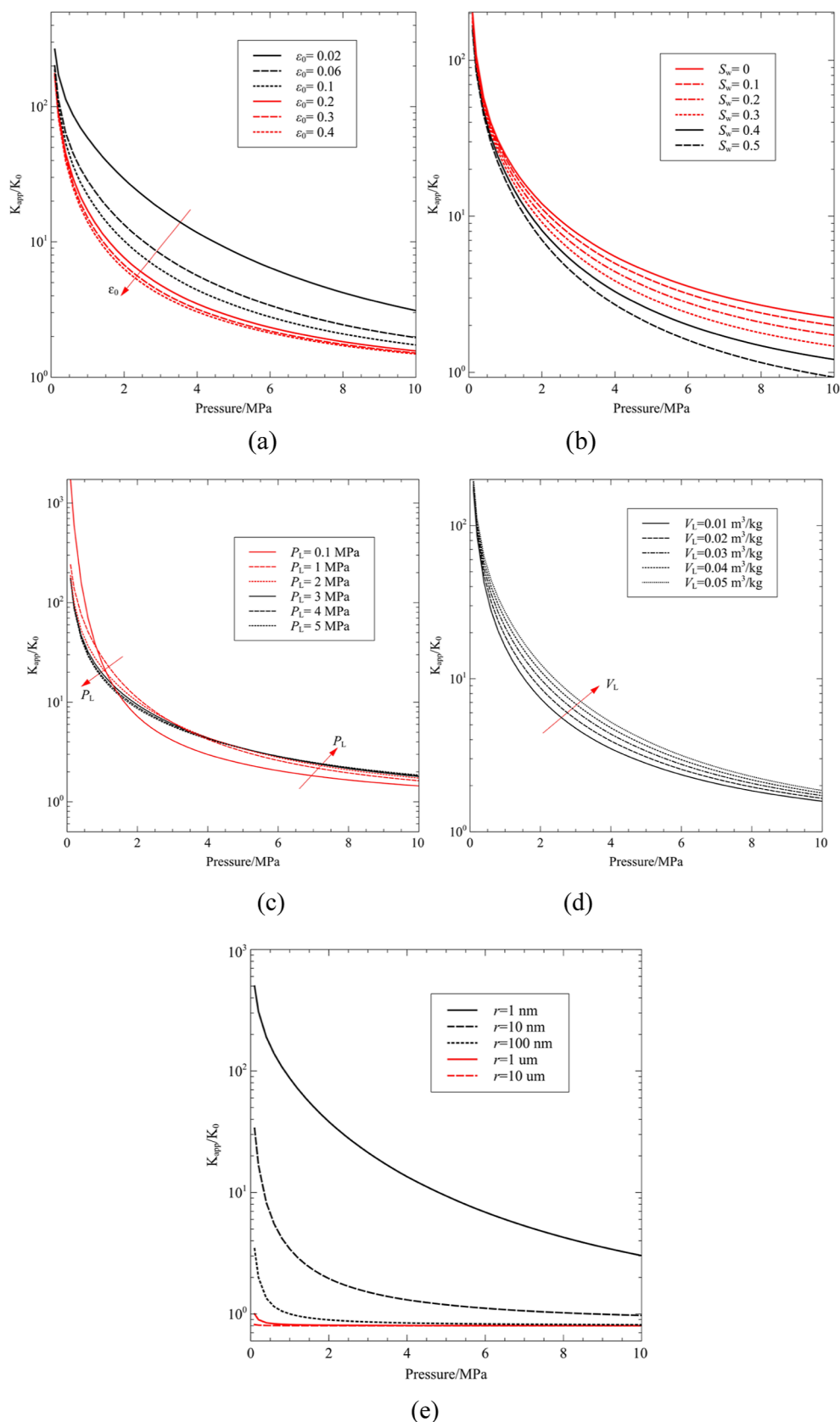
Figure 8. Variation of K_{app}/K_0 with pressure. (a) Under different initial porosities ε_0, (b) under different saturations S_w, (c) under different Langmuir pressures P_L, (d) under different Langmuir volumes V_L, and (e) under different average pore radii r.

8d. The permeability of porous media is closely related to its equivalent pore radius, and the effect of equivalent pore size on

K_{app} is similar to that of initial porosity. There is no doubt that the larger the equivalent pore size, the higher the K_{app}, but the

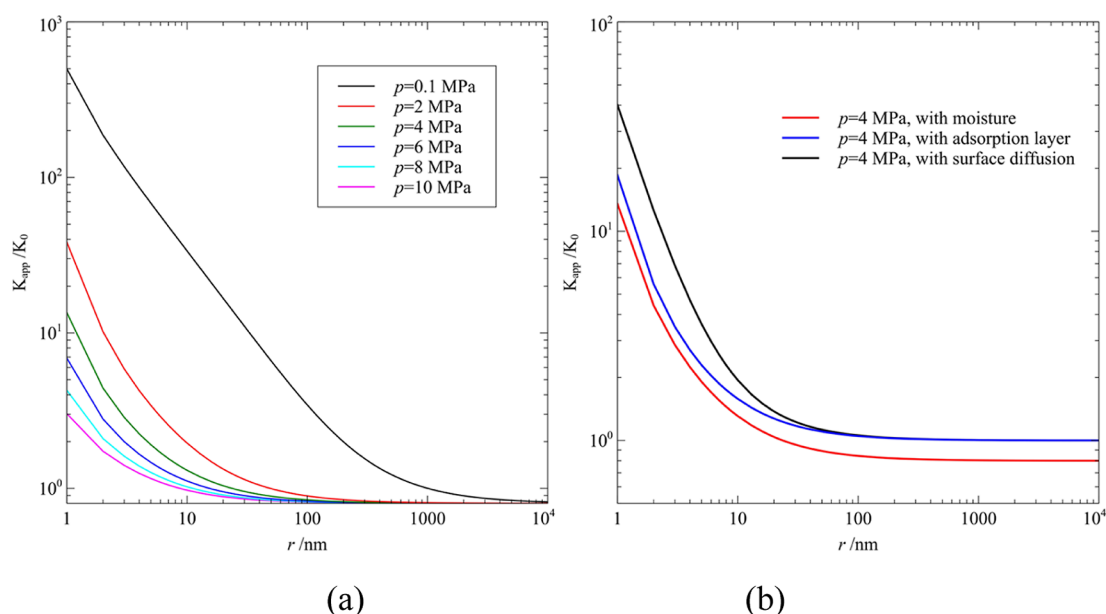(a)   (b)

Figure 9. Variation of K_{app}/K_0 with average pore radius. (a) With moisture under different pressures and (b) considering different transport regimes under $p = 4$ MPa.

smaller the equivalent pore size, the larger the K_{app}/K_0, as shown in Figure 8e, indicating that the effect of moisture adsorption on K_{app} is greater at smaller equivalent pore sizes, and when r is larger than 100 nm, the effect of moisture adsorption is negligible.

The equivalent pore size of typical CBM reservoirs is generally less than 100 nm or even less than 10 nm. Therefore, when modeling the methane transport behavior in moist coal, the results obtained may deviate significantly from the actual value if the effect of moisture adsorption is ignored.

Figure 9a shows the variations of K_{app}/K_0 with the equivalent pore radius r under different pressure conditions when considering moisture adsorption. The overall trend of K_{app}/K_0 decreases with the increase of pore radius under different pressure conditions. Theoretically, K_{app} grows with increasing r, but the non-Darcy effect depends on the pore size, i.e., the smaller the pore size, the more significant the effect resulting from Knudsen diffusion and surface diffusion, and the higher the proportion of adsorption layers of gas and moisture in the gas transport channel. With higher pressure, the magnitude of the initial value of K_{app}/K_0 is smaller. It means that K_{app} is closer to K_0. That is because the larger p is, the smaller the Kn number is, which makes the gas transport behavior tend to be in viscous flow. The contribution of Knudsen diffusion and surface diffusion to the total flux weakens, and the effect of molecular and moisture absorption layers is stronger under high-pressure conditions. When $p > 2$ MPa, if $r > 100$ nm, the change of K_{app}/K_0 is small, and it can be negligible when the pressure changes.

Figure 9b shows the variations of K_{app}/K_0 with the equivalent pore radius r for step application of the effects of surface diffusion, the molecular adsorption layer, and the moisture adsorption layer. The global trend shows that the initial value of K_{app}/K_0 is smaller when the gas adsorption effect is considered, and this value drops further when the effect of moisture adsorption is considered additionally. In macropores, i.e., $r > 100$ nm, the tendency of K_{app}/K_0 when gas adsorption is considered almost overlaps with the results when only surface diffusion is included, while K_{app}/K_0 remains more decaying than the previous two cases when moisture adsorption is further

considered. It suggests that the non-Darcy effect caused by gas adsorption in macropores is negligible, while that of moisture adsorption cannot be neglected.

4. CONCLUSIONS

In this paper, we developed an apparent permeability model for coalbed methane migration in moisture coal which coupled viscous flow, Knudsen diffusion, and surface diffusion and considered the effects of adsorbed gas molecules and moisture on the pore space. We have analyzed the relationship between the characteristic parameters of moist coal and compared the results of the present model with those of previous research to validate its accuracy. The model was then used to study the evolution of the apparent permeability of coalbed methane under varying pressure conditions and pore size distributions.

The main findings are as follows:

(1) The moisture content (ω) increases with the growth of saturation (S_w). When the porosity (ε) is small, the increasing rate of ω is slow, while for $\varepsilon > 0.1$, the increasing rate of ω is greatly accelerated and shows non-linear features. Typical coal seams usually have a porosity of less than 0.1, and the moisture content is linearly and positively related to saturation.

(2) Gas adsorption in the pores drops the apparent permeability, which can be further weakened by moisture adsorption under high-pressure conditions, while the effect of moisture adsorption becomes negligible at pressures below 1 MPa.

(3) In moist coal, higher water saturation (S_w) weakens gas transport capacity. When $S_w = 0.6$, the effective area of gas transport channels is only 48.8% of the initial value. The effect of moisture adsorption on gas transport is more significant with smaller pore sizes ($r < 10$ nm), and the pore space occupied by moisture adsorption can reach 10.9% of the total pore volume. As the initial porosity is greater, K_{app} becomes higher, but K_{app}/K_0 will be smaller, indicating a weaker non-Darcy effect. The effect of adsorbed moisture causes the Langmuir volume (V_L) to

decay with increasing pressure, but K_{app}/K_0 maintains the trend of increasing with V_L. While the cases of Langmuir pressure (P_L) are more complicated. Under a low-pressure condition, the smaller the Langmuir pressure, the larger the non-Darcy effect. However, with the increase of pressure, the non-Darcy effect weakens, and under high-pressure conditions, it may even appear to have an opposite tendency to low-pressure.

(4) The non-Darcy effect weakens with the increase of the average pore radius, and the non-Darcy effect under the influence of moisture adsorption is slightly smaller compared to that without considering moisture adsorption. The average pore size of typical coalbed methane reservoirs is mostly less than 100 nm or even less than 10 nm; therefore, the results obtained for modeling the methane transport behavior in moist coalbeds may deviate significantly from the actual values if the effect of moisture adsorption is neglected.

The present permeability model can capture the transport characteristics of CBM in moist coal seams more realistically and is more applicable for predicting and evaluating the gas transport performance under dynamic variations of pressure, pore size, and moisture. The results in this paper can explain the transport behavior of gas in moist, tight, porous media and also provide a foundation for coalbed methane permeability evaluation.

■ DATA AVAILABILITY

The data used to support the findings of this study are included in the article.

■ AUTHOR INFORMATION

Corresponding Author

Zhigao Peng − *College of Civil Engineering, Hunan City University, Yiyang 413000, China; Hunan Engineering Research Center of Structural Safety and Disaster Prevention for Urban Underground Infrastructure, Hunan City University, Yiyang 413000, China;* ⓘ orcid.org/0000-0002-2695-2531; Email: pengzhgg@163.com

Authors

Shenggui Liu − *School of Mechanics & Civil Engineering, China University of Mining and Technology (Beijing), Beijing 100083, China*

Zongwei Deng − *College of Civil Engineering, Hunan City University, Yiyang 413000, China*

Haoxiong Feng − *College of Civil Engineering, Hunan City University, Yiyang 413000, China*

Ming Xiao − *College of Civil Engineering, Hunan City University, Yiyang 413000, China*

Complete contact information is available at:
https://pubs.acs.org/10.1021/acsomega.3c01152

Notes

The authors declare no competing financial interest.

■ ACKNOWLEDGMENTS

■ REFERENCES

(1) Beskok, A.; Karniadakis, G. E. Report: A Model for Flows in Channels, Pipes, and Ducts at Micro and Nano Scales. *Microscale Thermophys. Eng.* **1999**, *3*, 43−77.

(2) Xiong, X.; Devegowda, D.; Michel Villazon, G. G.; Sigal, R. F.; Civan, F. A Fully-Coupled Free and Adsorptive Phase Transport Model for Shale Gas Reservoirs Including Non-Darcy Flow Effects. In *SPE Annual Technical Conference and Exhibition*; Society of Petroleum Engineers: San Antonio, Texas, USA, 2012.

(3) Freeman, C. M.; Moridis, G. J.; Blasingame, T. A. A Numerical Study of Microscale Flow Behavior in Tight Gas and Shale Gas Reservoir Systems. *Transp. Porous Media* **2011**, *90*, 253−268.

(4) Kang, S. M.; Fathi, E.; Ambrose, R. J.; Akkutlu, I. Y.; Sigal, R. F. Carbon Dioxide Storage Capacity of Organic-Rich Shales. *SPE J.* **2011**, *16*, 842−855.

(5) Wu, K.; Li, X.; Guo, C.; Wang, C.; Chen, Z. A Unified Model for Gas Transfer in Nanopores of Shale-Gas Reservoirs: Coupling Pore Diffusion and Surface Diffusion. *SPE J.* **2016**, *21*, 1583−1611.

(6) Wu, K.; Chen, Z.; Li, X.; Guo, C.; Wei, M. A Model for Multiple Transport Mechanisms through Nanopores of Shale Gas Reservoirs with Real Gas Effect−Adsorption-Mechanic Coupling. *Int. J. Heat Mass Transfer* **2016**, *93*, 408−426.

(7) Wang, J.; Chen, L.; Kang, Q.; Rahman, S. S. Apparent Permeability Prediction of Organic Shale with Generalized Lattice Boltzmann Model Considering Surface Diffusion Effect. *Fuel* **2016**, *181*, 478−490.

(8) Ning, Y.; He, S. Permeability Prediction Considering Surface Diffusion for Gas Shales by Lattice Boltzmann Simulations on Multi-Scale Reconstructed Digital Rocks. In *International Petroleum Technology Conference*; 2016; p 22.

(9) Sun, H.; Yao, J.; Fan, D.; Wang, C.; Sun, Z. Gas Transport Mode Criteria in Ultra-Tight Porous Media. *Int. J. Heat Mass Transfer* **2015**, *83*, 192−199.

(10) Peng, Z.; Liu, S.; Li, Y.; Yao, Q. Apparent Permeability Prediction of Coal Matrix with Generalized Lattice Boltzmann Model Considering Non- Darcy Effect. *Geofluids* **2020**, *2020*, 1−14.

(11) Peng, Z.; Deng, Z.; Feng, H.; Liu, S.; Li, Y. Multiscale Lattice Boltzmann Simulation of the Kinetics Process of Methane Desorption-Diffusion in Coal. *ACS Omega* **2021**, *6*, 19789−19798.

(12) Busch, A.; Gensterblum, Y. CBM and CO2-ECBM Related Sorption Processes in Coal: A Review. *Int. J. Coal Geol.* **2011**, *87*, 49−71.

(13) Gensterblum, Y.; Merkel, A.; Busch, A.; Krooss, B. M. High-Pressure CH4 and CO2 Sorption Isotherms as a Function of Coal Maturity and the Influence of Moisture. *Int. J. Coal Geol.* **2013**, *118*, 45−57.

(14) Joubert, J. I.; Grein, C. T.; Bienstock, D. Sorption of Methane in Moist Coal. *Fuel* **1973**, *52*, 181−185.

(15) Wang, L.; Chen, E.; Liu, S.; Cheng, Y.; Cheng, L.; Chen, M.; Guo, H. Experimental Study on the Effect of Inherent Moisture on Hard Coal Adsorption−Desorption Characteristics. *Adsorption* **2017**, *23*, 723−742.

(16) Chen, M.; Cheng, Y.; Li, H.; Wang, L.; Jin, K.; Dong, J. Impact of Inherent Moisture on the Methane Adsorption Characteristics of Coals with Various Degrees of Metamorphism. *J. Nat. Gas Sci. Eng.* **2018**, *55*, 312−320.

(17) Hao, M.; Wei, C.; Qiao, Z. Effect of Internal Moisture on CH4 Adsorption and Diffusion of Coal: A Molecular Simulation Study. *Chem. Phys. Lett.* **2021**, *783*, 139086.

(18) Zhang, Q.; Liu, X.; Nie, B.; Wu, W.; Wang, R. Methane Sorption Behavior on Tectonic Coal under the Influence of Moisture. *Fuel* **2022**, *327*, 125150.

(19) Chen, M.; Masum, S.; Thomas, H. Modeling Adsorption and Transport Behavior of Gases in Moist Coal Matrix. *Energy Fuel.* **2021**, *35*, 13200−13214.

(20) Pajdak, A. Studies on the Influence of Moisture on the Sorption and Structural Properties of Hard Coals. *Int. J. Greenh. Gas Control* **2020**, *103*, 103193.

(21) Laxminarayana, C.; Crosdale, P. J. Controls on Methane Sorption Capacity of Indian Coals. *AAPG Bull.* **2002**, *86*, 201−212.

(22) Day, S.; Sakurovs, R.; Weir, S. Supercritical Gas Sorption on Moist Coals. *Int. J. Coal Geol.* **2008**, *74*, 203−214.

(23) Guo, H.; Cheng, Y.; Wang, L.; Lu, S.; Jin, K. Experimental Study on the Effect of Moisture on Low-Rank Coal Adsorption Characteristics. *J. Nat. Gas Sci. Eng.* **2015**, *24*, 245−251.

(24) Zhao, Y.; Liu, S.; Elsworth, D.; Jiang, Y.; Zhu, J. Pore Structure Characterization of Coal by Synchrotron Small-Angle X-Ray Scattering and Transmission Electron Microscopy. *Energy Fuels* **2014**, *28*, 3704−3711.

(25) Cai, Y.; Liu, D.; Pan, Z.; Yao, Y.; Li, J.; Qiu, Y. Pore Structure and Its Impact on CH4 Adsorption Capacity and Flow Capability of Bituminous and Subbituminous Coals from Northeast China. *Fuel* **2013**, *103*, 258−268.

(26) Hou, S.; Wang, X.; Wang, X.; Yuan, Y.; Pan, S.; Wang, X. Pore Structure Characterization of Low Volatile Bituminous Coals with Different Particle Size and Tectonic Deformation Using Low Pressure Gas Adsorption. *Int. J. Coal Geol.* **2017**, *183*, 1−13.

(27) Li, Y.; Zhang, C.; Tang, D.; Gan, Q.; Niu, X.; Wang, K.; Shen, R. Coal Pore Size Distributions Controlled by the Coalification Process: An Experimental Study of Coals from the Junggar, Ordos and Qinshui Basins in China. *Fuel* **2017**, *206*, 352−363.

(28) Chen, Y.; Tang, D.; Xu, H.; Tao, S.; Li, S.; Yang, G.; Yu, J. Pore and Fracture Characteristics of Different Rank Coals in the Eastern Margin of the Ordos Basin, China. *J. Nat. Gas Sci. Eng.* **2015**, *26*, 1264−1277.

(29) Peng, Z.; Liu, S.; Li, Y.; Deng, Z.; Feng, H. Pore-Scale Lattice Boltzmann Simulation of Gas Diffusion−Adsorption Kinetics Considering Adsorption-Induced Diffusivity Change. *Energies* **2020**, *13*, 4927.

(30) Li, J.; Li, X.; Wu, K.; Chen, Z. J.; Wang, K.; Zhong, M.; Bai, Z. Methane Transport through Nanoporous Shale with Sub-Irreducible Water Saturation. Day 3 Wed, June 14, 2017; SPE: Paris, France, 2017; p D031S007R005.

(31) Ozdemir, E.; Schroeder, K. Effect of Moisture on Adsorption Isotherms and Adsorption Capacities of CO_2 on Coals. *Energy Fuels* **2009**, *23*, 2821−2831.

(32) Javadpour, F.; Fisher, D.; Unsworth, M. Nanoscale Gas Flow in Shale Gas Sediments. *J. Can. Pet. Technol.* **2007**, *46*(), DOI: 10.2118/07-10-06,

(33) Klinkenberg, L. J. The Permeability of Porous Media to Liquids and Gases. In *Drilling and production practice*; American Petroleum Institute, 1941.

(34) Civan, F. Effective Correlation of Apparent Gas Permeability in Tight Porous Media. *Transp. Porous Media* **2010**, *82*, 375−384.

(35) Roy, S.; Raju, R.; Chuang, H. F.; Cruden, B. A.; Meyyappan, M. Modeling Gas Flow through Microchannels and Nanopores. *J. Appl. Phys.* **2003**, *93*, 4870−4879.

(36) Javadpour, F. Nanopores and Apparent Permeability of Gas Flow in Mudrocks (Shales and Siltstone). *J. Can. Pet. Technol.* **2009**, *48*, 16−21.

(37) Do, H. D.; Do, D. D.; Prasetyo, I. On the Surface Diffusion of Hydrocarbons in Microporous Activated Carbon. *Chem. Eng. Sci.* **2001**, *56*, 4351−4368.

(38) Chen, Y. D.; Yang, R. T. Concentration Dependence of Surface Diffusion and Zeolitic Diffusion. *AIChE J.* **1991**, *37*, 1579−1582.

(39) Darabi, H.; Ettehad, A.; Javadpour, F.; Sepehrnoori, K. Gas Flow in Ultra-Tight Shale Strata. *J. Fluid Mech.* **2012**, *710*, 641−658.

(40) Tang, W.; Zhang, S.; Dong, J.; Guo, X. *Coal Conversion* **2015**, *38*, 5−9.

(41) Wang, C.; Chen, L.-J.; Wang, C.-S.; Zhang, X.-H. Experiment on Thermal-Induced Expansion and Mechanical Properties of Gas-Bearing Intact Coal Subjected to Thermal-Mechanical Loading. *Rock Soil Mech.* **2014**, *35*, 1015−1024.